Published in final edited form as:

Nat Med. 2018 August ; 24(8): 1246–1256. doi:10.1038/s41591-018-0092-9.

Senolytics Improve Physical Function and Increase Lifespan in Old Age

Ming Xu[1,10,*], **Tamar Pirtskhalava**[1], **Joshua N. Farr**[1], **Bettina M. Weigand**[1,2], **Allyson K. Palmer**[1], **Megan M. Weivoda**[1], **Christina L. Inman**[1], **Mikolaj B. Ogrodnik**[1,2], **Christine M. Hachfeld**[1], **Daniel G. Fraser**[1], **Jennifer L. Onken**[1], **Kurt O. Johnson**[1], **Grace C. Verzosa**[1], **Larissa G. P. Langhi**[1], **Moritz Weigl**[1], **Nino Giorgadze**[1], **Nathan K. LeBrasseur**[1], **Jordan D. Miller**[1], **Diana Jurk**[2], **Ravinder J. Singh**[3], **David B. Allison**[4], **Keisuke Ejima**[4], **Gene B. Hubbard**[5], **Yuji Ikeno**[5,6], **Hajrunisa Cubro**[7], **Vesna D. Garovic**[7], **Xiaonan Hou**[8], **SJ Weroha**[8], **Paul D. Robbins**[9], **Laura J. Niedernhofer**[9], **Sundeep Khosla**[1], **Tamara Tchkonia**[1,*], and **James L. Kirkland**[1,*]

[1]Robert and Arlene Kogod Center on Aging, Mayo Clinic, 200 First St., S.W., Rochester, MN 55905, USA

[2]Newcastle University Institute for Ageing and Institute for Cell and Molecular Biosciences, Newcastle University, Newcastle Upon Tyne, NE2 4HH, UK

[3]Department of Laboratory Medicine and Pathology, Mayo Clinic, 200 First St., S.W., Rochester, MN 55905, USA

[4]Department of Epidemiology & Biostatistics, School of Public Health, Indiana University-Bloomington and Nathan Shock Center on Comparative Energetics and Aging, University of Alabama at Birmingham, 1025 E 7th St, Bloomington, IN 47405, USA

[5]Barshop Institute for Longevity and Aging Studies and Department of Pathology, University of Texas Health Science Center at San Antonio, 15355 Lambda Drive, San Antonio, TX 78245, USA

[*]To whom correspondence should be addressed at: Mayo Clinic Robert and Arlene Kogod Center on Aging, 200 First St., S.W., Rochester, MN 55905, Telephone: (507) 266-9151, Fax: (507) 293-3853, kirkland.james@mayo.edu; xu.ming@mayo.edu (mixu@uchc.edu, after 6/8/2018); tchkonia.tamar@mayo.edu.
Note: Ming Xu will move to University of Connecticut Center on Aging after 6/8/2018. The email will be changed to mixu@uchc.edu by then.

Author contributions: M.X., T.T., and J.L.K. conceived and designed the study. M.X. performed and analyzed most of the transplanted animal experiments and human adipose tissue explant experiments. N.G. and T.T. contributed to the human adipose tissue explant experiments. J.N.F., D.G.F., J.L.O., and S.K. contributed to the study of aged mice treated with senolytics. A.K.P. contributed to the bioluminescence studies. M.B.O. and D.J. contributed to ear fibroblast isolation. T.P., M.X., T.T., and C.L.I. performed the survival experiments using senolytics in aged mice. B.M.W., M.M.W., C.M.H., N.K.L., H.C., V.D.G., X.H., S.J.W., K.O.J., M.W., L.G.P.L., G.C.V., N.K.L., P.D.R., L.J.N., and J.D.M. contributed to the animal studies. R.J.S. contributed to androgen measurement. D.B.A. and K.E. contributed to lifespan analysis. G.B.H. and Y.I. contributed to mouse pathology analysis. M.X. and J.L.K. wrote the manuscript with input from all co-authors. J.L.K., M.X., and T.T. oversaw all experimental design, data analysis, and manuscript preparation.

Competing financial interests: J.L.K, T.T., M.X., T.P., N.G., and A.K.P. have a financial interest related to this research. Patents on senolytic drugs (PCT/US2016/041646) are held by Mayo Clinic. This research has been reviewed by the Mayo Clinic Conflict of Interest Review Board and was conducted in compliance with Mayo Clinic Conflict of Interest policies. None of the other authors has a relevant financial conflict of interest.

[6]Geriatric Research Education and Clinical Center, South Texas Veterans Healthcare System, 15355 Lambda Drive, San Antonio, TX 78245, USA

[7]Department of Internal Medicine, Division of Nephrology and Hypertension, Mayo Clinic, 200 First St., S.W., Rochester, MN 55905, USA

[8]Department of Oncology, Mayo Clinic, 200 First St., S.W., Rochester, MN 55905, USA

[9]Department of Molecular Medicine, Center on Aging, The Scripps Research Institute, 130 Scripps Way, Jupiter, FL 33458, USA

[10]University of Connecticut Center on Aging, UConn Health, 263 Farmington Avenue, Farmington, CT 06030, USA (after 6/8/2018)

Abstract

Physical function declines in old age, portending disability, increased health expenditures, and mortality. Cellular senescence, leading to tissue dysfunction, may contribute to these consequences of aging, but whether senescence can directly drive age-related pathology and be targeted therapeutically is still unclear. Here we demonstrate that transplanting relatively small numbers of senescent cells into young mice is sufficient to cause persistent physical dysfunction, as well as to spread cellular senescence to host tissues. Transplanting even fewer senescent cells had the same effect in older recipients, accompanied by reduced survival, indicating the potency of senescent cells in shortening health- and life-span. The senolytic cocktail, dasatinib plus quercetin, which causes selective elimination of senescent cells, decreased the number of naturally-occurring senescent cells and their secretion of frailty-related pro-inflammatory cytokines in explants of human adipose tissue. Moreover, intermittent oral administration of senolytics to both senescent cell-transplanted younger and naturally-aged mice alleviated physical dysfunction and increased post-treatment survival by 36% while reducing mortality hazard to 65%. Our study provides proof-of-concept evidence that senescent cells can cause physical dysfunction and decreased survival even in young mice, while senolytics can enhance remaining health- and lifespan in old mice.

Keywords

aging; cellular senescence; frailty; dasatinib; quercetin

Introduction

New approaches to treat age-related diseases (*e.g.*, cardiovascular disease) may yield lifespan extension, but potentially at the cost of extending late-life morbidity[1]. A major question in biology is whether interventions can be devised that enhance healthspan in tandem with increasing remaining lifespan, so that the period of morbidity near the end of life is not increased[2]. Physical dysfunction and incapacity to respond to stresses[3,4] become increasingly prevalent toward the end of life[5], with up to 45% of people over the age of 85 being frail[6]. This physical dysfunction is associated with considerable morbidity, including decreased mobility and increased burden of age-related chronic diseases, loss of independence, nursing home and hospital admissions, and mortality[7]. The cellular pathogenesis of age-related physical dysfunction has not been fully elucidated and there are

currently no root cause-directed, mechanism-based interventions for improving physical function in the elderly available for clinical application. Here, we report a potential strategy for addressing this need: reducing senescent cell burden.

Cellular senescence is a cell fate involving extensive changes in gene expression and proliferative arrest. Senescence can be induced by such stresses as DNA damage, telomere shortening, oncogenic mutations, metabolic and mitochondrial dysfunction, and inflammation[8–10]. Senescent cell burden increases in multiple tissues with aging[11], at sites of pathology in multiple chronic diseases, and after radiation or chemotherapy[12]. Senescent cells can secrete a range of pro-inflammatory cytokines, chemokines, proteases, and other factors termed the senescence-associated secretory phenotype (SASP)[13,14], which contributes to local and systemic dysfunction with aging and in a number of diseases[15–21]. A month or more of continuous treatment with JAK1/2 inhibitors or rapamycin can enhance function in older mice[14,22]. However, JAK1/2 inhibitors and rapamycin have an extensive range of effects on cellular function. Among these is reduced production of some SASP components. Based on these points, we hypothesized that senescent cells might potentially contribute to age-related physical dysfunction and, if so, that targeting them therapeutically could improve lifespan and healthspan.

Results

Transplanting small numbers of senescent cells is sufficient to induce physical dysfunction in young mice

To test if senescent cells can directly cause physical dysfunction, we first transplanted senescent (SEN) or control, non-senescent (CON) preadipocytes (also termed adipocyte progenitors or adipose-derived stem cells[23]) isolated from luciferase-expressing transgenic (LUC^+) mice intraperitoneally into syngeneic, young (6-month-old) wild type (WT) animals (Fig. 1a). We induced cellular senescence using 10 Gray (Gy) radiation, which resulted in more than 85% of cells becoming senescent (Supplementary Fig. 1a,b). We transplanted preadipocytes because: 1) the SASP of radiation-induced senescent mouse preadipocytes (Supplementary Fig. 1c,d) resembles that of endogenous senescent cells with aging (Supplementary Fig. 1e)[20,24] and in idiopathic pulmonary fibrosis[25]; 2) preadipocytes are less immunogenic or subject to rejection than other cell types[26]; and 3) these cells are arguably the most abundant type of progenitors in humans[27] that are subject to cellular senescence. We also used doxorubicin to induce senescence to ascertain if the physiological impact of transplanted senescent cells is limited to the context of radiation-induced senescence: senescent cells induced by doxorubicin developed a SASP similar to that of radiation-induced senescent cells (Supplementary Fig. 1f). Five days after intraperitoneal transplantation of SEN or CON preadipocytes, the cells were mainly located in visceral fat (Fig. 1b,c and Supplementary Fig. 2a,b). Both the SEN and CON transplanted cells remained detectable by *in vivo* bioluminescence imaging (BLI) for up to 40 days (Supplementary Fig. 2c). Of note, we observed that senescent cells had higher luciferase activity than control non-senescent cells, even though they were from the same LUC transgenic mice (Supplementary Fig.2d).

To determine whether the transplanted senescent cells induced physical dysfunction in these mice as reflected by criteria used in clinical practice[4], we measured maximal walking speed (RotaRod), muscle strength (grip strength), physical endurance (hanging test and treadmill), daily activity, food intake, and body weight. Previously healthy young adult mice transplanted with 10^6 SEN cells had significantly lower maximal walking speed, hanging endurance, and grip strength by one month after transplantation compared to mice transplanted with CON cells (Fig 1d-f and Supplementary Fig. 3a). Transplanting the same number of CON cells had no effect compared to injecting phosphate-buffered saline (PBS). Daily activity, treadmill performance, food intake and body weight were not statistically different among groups (Fig. 1g-j). Transplanting 0.5×10^6 SEN cells was sufficient to cause decreased grip strength (Fig. 1f) and maximal walking speed (Supplementary Fig. 3b), while transplanting 0.2×10^6 senescent cells had no detectible effects. Thus, SEN cells can impair physical function in a dose-dependent manner. We estimate that 6-month-old mice have $7\text{-}8 \times 10^9$ cells of all types and the total cell number in intraperitoneal adipose tissue, where the transplanted cells were mainly located (Supplementary Fig. 2b), is $\sim 3.5\text{-}6 \times 10^8$ cells (**Online methods**). Thus in young mice if only 1 cell in 7,000 to 15,000 (0.01% to 0.03%) throughout the body, or 1 cell in 350 (0.28%) locally is a transplanted senescent cell, important age-related phenotypes ensue.

Reduced walking speed began as early as 2 weeks following a single implantation of SEN cells (Supplementary Fig. 3c) and persisted for up to 6 months (Supplementary Fig. 3d), yet the transplanted cells survived *in vivo* for only approximately 40 days, consistent with the possibility that senescent cells might induce senescence in normal host cells[28,29]. We therefore tested if senescent cells can indeed cause other cells to become senescent *in vivo* by transplanting constitutively LUC-expressing SEN cells and determining whether senescence occurs in the LUC-negative recipients' tissue. Visceral fat was where most of the transplanted LUC^+ senescent cells resided (Supplementary Fig. 2b). Two months after transplantation, we found more senescence-associated β-galactosidase $(SA\text{-}\beta gal)^+$ cells and higher CDKN2A ($p16^{Ink4a}$) expression in visceral adipose tissue from SEN than CON cell-transplanted mice (Fig. 1k,l), beyond the time the transplanted senescent cells were present as reflected by luciferase signal (Supplementary Fig. 2c). Telomere-associated foci (TAFs) are sites of DNA damage within telomeres[30]. TAFs appear to be a more specific marker of senescence than some others, such as SA-βgal. Significantly more TAF^+ cells were found in visceral adipose tissue of mice that had been injected with SEN than CON cells (Fig. 1m). These TAF^+ cells were LUC^-, so they were the recipients' own cells and not transplanted cells. $F4/80^+$ macrophage accumulation was not induced in adipose tissue by the intraperitoneal SEN cell transplantation (Supplementary Fig. 3e,f). Consistent with spread of senescence not only locally but also to distant tissues, expression of the markers and mediators of senescence, $p16^{Ink4a}$, *tumor necrosis factor (TNF)α*, and *interleukin(IL)-6*, was higher in the quadriceps muscles of SEN- than CON-transplanted mice (Supplementary Fig. 4a), a tissue where transplanted cells were not detected (Supplementary Fig. 2b). Similarly to adipose tissue, $F4/80^+$ macrophage accumulation was not induced in muscle by SEN cell transplantation (Supplementary Fig. 4b). Thus, senescence spreading may explain how a small number of transplanted senescent cells caused such profound, long-lasting, and deleterious systemic effects.

To test further whether SASP-related factors can contribute to induction of cellular senescence *in vivo*, we examined IL-10 knock-out mice, which have a genetically-induced premature pro-inflammatory phenotype that resembles the SASP and which also prematurely develop physical dysfunction reminiscent of human frailty[31]. We found that these animals do indeed have more senescent cells than wildtype controls, in support of the possibility that the SASP can induce senescence spreading *in vivo* (Supplementary Fig. 5a-c).

Aging and high-fat diet exacerbate effects of senescent cell transplantation

Because aging is associated with senescent cell accumulation[14], we tested if increased recipient age potentiates the effects of transplanting senescent cells. We transplanted 0.5×10^6 SEN or CON preadipocytes into older (17-month) mice, so that 0.007% of all cells in the recipients were transplanted SEN or CON cells, and one month later we measured various parameters of physical function (Fig. 2a). We found that mice transplanted with SEN cells had lower maximal walking speed, hanging endurance, and grip strength compared to CON mice (Fig. 2b-d). These findings were consistent across several independent cohorts of male (Supplementary Fig. 6a-f) and female mice (Supplementary Fig. 6g-l). Body weight, treadmill performance, daily activity, and food intake were not statistically different after transplanting SEN cells into the older mice (Fig. 2e-h). Transplanting 0.5×10^6 SEN cells led to greater impairment in walking speed and hanging endurance in 17-month-old mice than 6-month-old mice (Fig. 2i), while other parameters showed no statistically significant difference. Notably, in the 17 month-old mice transplanted with SEN cells, survival for the following year was significantly lower than that of age-matched CON mice, with a 5.2 fold higher risk of death (mortality hazard ratio, $P = 0.006$) (Fig. 2j). Tumor burden, disease burden at death, and causes of death were not significantly altered by SEN cell transplantation compared to CON cells (Fig. 2k,l), suggesting that a small number of senescent cells may shorten survival through a general process, such as hastening the progression of aging, rather than by inducing any one or a few individual diseases. Thus, augmenting senescent cell burden induces physical dysfunction, more so in middle-aged than younger individuals, and increases mortality.

To determine whether augmenting senescent cell burden reduces resilience in the face of high fat intake, which is a metabolic stress known to promote senescent cell accumulation[32], SEN or CON preadipocytes were transplanted into 8-month-old non-obese mice and then fed a high-fat diet (HFD) for one month, followed by measurements of physical function (Fig. 3a). The HFD-fed mice transplanted with 0.4×10^6 SEN cells had lower maximal walking speed, hanging endurance, grip strength, daily activity, and food intake compared to HFD-fed mice transplanted with 0.4×10^6 CON cells (Fig. 3b-f). Body weight and treadmill performance were not statistically different (Fig. 3g,h). SEN cell-transplanted mice on the HFD had more impairment in walking speed and hanging endurance than age-matched transplanted mice on a normal chow diet (NCD), while other parameters were not statistically significantly changed (Fig. 3i). Collectively, these data indicate that transplanting small numbers of senescent cells causes greater systemic dysfunction in older individuals or in the context of metabolic stress.

To test if the physical dysfunction in mice transplanted with SEN cells was due to transplant rejection, we transplanted mice with autologous ear fibroblasts in which senescence had been induced by 10 Gy radiation[16] *vs.* sham-radiated CON cells. Senescent fibroblasts[16] have a similar SASP to senescent preadipocytes (Supplementary Fig. 1c). 10^6 SEN or CON cells were transplanted back into the same mice from which the ear fibroblasts had been isolated and the mice were put on a HFD for 1 month (Fig. 3j). Transplanting autologous SEN ear fibroblasts intraperitoneally, compared to CON cells, led to impaired maximal walking speed, hanging endurance, and grip strength (Fig. 3k-q), as had occurred after transplanting non-autologous senescent preadipocytes. Moreover, we transplanted radiation-induced SEN primary human preadipocytes (characterized in[14]) *vs.* sham-radiated CON cells into severe combined immunodeficiency-beige (SCID-beige) mice with impaired T cell, B cell, and natural killer cell function[33]. Similarly to the effect of mouse senescent cells on immune-competent mice, we found physical function was impaired in the immune-deficient mice transplanted with the human SEN cells compared to those treated with CON cells or with PBS (Supplementary Fig. 7). Combined with our finding that SEN and CON cells persisted for the same amount of time after transplantation (Supplementary Fig. 2c), these data support the possibility that physical dysfunction did not arise principally as a consequence of transplant immune rejection or in response to a particular type of SEN cell.

D+Q reduces senescent cell burden and decreases pro-inflammatory cytokine secretion in human adipose tissue

Based on our finding that senescent cells cause physical dysfunction and shorten survival, senolytic agents, which can selectively eliminate senescent cells, might be an approach for enhancing healthspan in old individuals. Senolytic drugs have been reported to alleviate a variety of age-related disorders (reviewed in[34]). These agents were originally selected based on their ability to transiently disable the senescence-associated anti-apoptotic pathways (SCAPs) that protect senescent cells from their pro-apoptotic microenvironment[35]. However, the efficacy of senolytics in human tissues remains unclear. To begin the process of gauging the translational potential of this approach, we determined if the combination of dasatinib plus quercetin (D+Q), the first senolytics reported[35], is effective in a human tissue. We did so using freshly-isolated human omental adipose tissue obtained from obese individuals (BMI 45.5±9.1 kg/m^2; age 45.7±8.3 years), since obesity is associated with senescent cell accumulation[27,32]. The surgically excised explants, which indeed contained naturally-occurring senescent cells (Supplementary Fig. 8a), were immediately treated with D+Q (1μM + 20μM) or vehicle (V) for 48 hours (Fig. 4a). The explants treated with D+Q had significantly less TAF^+, $p16^{INK4A}$-highly expressing, and SA-βgal$^+$ cells (Fig. 4b-d) and also more cells undergoing apoptosis (Fig.4e and Supplementary Fig. 8b) compared to V-treated explants from the same subjects. Forty eight hours of treatment with vehicle did not affect total and senescent cell numbers in these adipose tissue explants (Supplementary Fig. 8c). Notably, the three senescence markers, TAF, $p16^{INK4A}$, and SA-βgal, correlated with each other (Supplementary Fig. 8d).

We next examined whether D+Q had acute effects on macrophages in these explants. We co-stained for $p16^{INK4A}$ and F4/80. Only the $p16^{INK4A+}$; F4/80$^-$ cell population was lower in the explants treated with D+Q compared to V, while the numbers of $p16^{INK4A+}$;F4/80$^+$ or

$p16^{INK4A-}$;$F4/80^{+}$ cells were not affected significantly (Supplementary Fig. 9a). In addition, expression of CD68 and EMR1, two macrophage markers, was not altered acutely by D+Q in the adipose tissue explants (Supplementary Fig. 9b). These data suggest that D+Q has little direct effect on macrophages, including $p16^{INK4A+}$ macrophages.

SEN preadipocytes produce a variety of pro-inflammatory cytokines[14] and can also induce cytokine production by adipose tissue *in vitro* (Supplementary Fig. 10), potentially leading to amplification of adipose tissue inflammation. To test if D+Q decreases cytokine secretion by adipose tissue from obese individuals, we treated explants with D+Q or V for 48 hours then washed the explants. Conditioned medium (CM) was collected in the absence of drugs over the next 24 hours. We measured secreted protein levels in CM after D+Q treatment, and found less secretion of the key SASP components[14], IL-6, IL-8, monocyte chemotactic protein-1 (MCP-1), plasminogen activator inhibitor-1 (PAI-1), and granulocyte macrophage colony-stimulating factor (GM-CSF) in CM from the D+Q group compared to V, while two non-SASP-related factors, IL-10 and interferon (IFN)-γ[14], were not statistically significantly altered (Fig.4f and Supplementary Fig. 11a). Furthermore, secretion of two adipokines, adiponectin and adipsin (markers of adipose tissue function[36]), were not lower in D+Q group, excluding a non-specific effect of D+Q on protein secretion or overall cell viability (Fig. 4f). D+Q increased expression of PPARγ and CEBPα, two key transcription factors that are required for adipose tissue function through regulating adipogenesis and adipose tissue insulin responsiveness[15,37] (Fig. 4g). This parallels the induction of these key adipogenic factors that we previously reported after targeting cellular senescence either by clearing senescent cells genetically or inhibiting the SASP[15]. D+Q reduced cytokine production more extensively in the human adipose tissue explants than either D or Q alone (Supplementary Fig. 11b), consistent with the finding that D+Q targets a broader range of senescent cells than D or Q alone[35]. Of note, increases in IL-6 (ref. [38,39]), MCP-1 (ref. [40,41]), and $p16^{INK4a}$ (ref. [42,43]) are associated with frailty in humans. Thus, it appears that D +Q can kill naturally-occurring human senescent cells and can attenuate secretion of inflammatory cytokines associated with human age-related frailty.

Eliminating senescent cells both prevents and alleviates physical dysfunction induced by senescent cell transplantation

We tested if D+Q kills transplanted senescent cells *in vivo* by injecting SEN or CON preadipocytes that that constitutively express LUC (LUC^{+}) intraperitoneally into non-luciferase-expressing WT mice. The mice were treated immediately after transplantation with D+Q or vehicle (V) for 3 days (Fig. 5a). Luminescence was significantly lower in SEN cell-transplanted mice treated with D+Q compared to V, while no difference was observed following treatment of mice transplanted with LUC^{+} CON cells (Fig. 5b,c), confirming D+Q is senolytic *in vivo*. These findings further support the conclusion that D+Q can selectively kill senescent cells.

We ascertained if clearing transplanted SEN cells using D+Q prevents development of physical dysfunction. Treating young mice with D+Q at the time of SEN cell transplantation for 3 days attenuated the deteriorations in walking speed, hanging endurance, and grip strength that occurred 1 month later in vehicle-treated SEN cell-transplanted mice,

consistent with the possibility that D+Q are sufficient to prevent the physical dysfunction caused by SEN cells (Fig. 5d-f). D+Q also alleviated the physical dysfunction that occurred in mice 5 weeks following SEN cell transplantation (Fig. 5g). In the SEN cell-transplanted mice, a single course of 5 days of D+Q treatment improved physical function compared to V (Fig. 5h-j). This improvement was evident 2 weeks after D+Q treatment and lasted for several months (Supplementary Fig. 12a). At these two time points of D+Q administration (immediately *vs.* 5 weeks after transplantation), the beneficial effects of D+Q were comparable. Therefore, we speculate that the time of administration of senolytics may be flexible, potentially increasing their clinical utility. Because D+Q have elimination half-lives of <12 hours[44,45], this sustained improvement in physical function following a single course of D+Q treatment does not involve mechanisms that require continuous presence of the drugs, such as occupancy of a receptor or sustained effects on an enzyme. These findings suggest that the senolytic activity of D+Q is sufficient to attenuate senescent cell-induced physical dysfunction.

Clearance of senescent cells alleviates physical dysfunction and increases late-life survival without extending morbidity in aged mice

D+Q has been shown to decrease senescent cells in a variety of tissues in different situations, including aging[25,35,46–48]. To test the role of senescent cells in physical dysfunction in aged mice, we treated 20-month-old non-transplanted, wild-type mice with D +Q or V intermittently for 4 months (Fig. 6a). D+Q alleviated physical dysfunction, with higher maximal walking speed, hanging endurance, grip strength, treadmill endurance, and daily activity in mice treated with D+Q compared to V (Fig. 6b-g). Food intake also tended to be higher in D+Q treated mice ($P = 0.074$; Fig. 6h). Moreover, the expression of several key SASP components was lower in the visceral adipose tissue from aged mice treated with D+Q compared to V (Fig. 6i), concordant with lower secretion of SASP factors by human adipose tissue treated by D+Q (Fig. 4g).

To test further the possibility there could be a causal role for senescent cells in inducing physical dysfunction, we used the transgenic *INK-ATTAC* mouse model, in which endogenous $p16^{Ink4a+}$ cells, many of which are senescent, can be genetically cleared by activating the caspase-8 moiety of ATTAC, which is expressed only in $p16^{Ink4a+}$ cells[49] (see **Online Methods**). Consistent with our findings in mice treated with D+Q, reducing the burden of highly $p16^{Ink4a}$-expressing cells in 26-28 month old *INK-ATTAC*$^{+/-}$ mice also alleviated physical dysfunction (Supplementary Fig. 12b-f).

Testosterone has been reported to alleviate physical dysfunction with aging[50]. To test if testosterone levels are affected by D+Q, we measured circulating testosterone levels in two cohorts and found no statistically significant differences between the V and D+Q groups (Supplementary Fig. 13). This appears to rule out the potential explanation that improvement of physical function is due to increased testosterone induced by senolytics.

Next, we tested if eliminating senescent cells using a potentially translatable approach, intermittent treatment with senolytics beginning at very old age, extends remaining lifespan in wild-type mice (Fig. 6j). Remarkably, mice with bi-weekly administration of D+Q starting at 24-27 months of age (equivalent to age 75-90 years in humans) had 36% higher

median post-treatment lifespan and lower mortality hazard, 64.9% ($P = 0.01$), compared to the vehicle group (Fig. 6k,l and Supplementary Fig.14a,b), indicating that senolytics can reduce risk of death in old mice.

To test if this reduced mortality in old mice comes at the cost of an increased period of late-life morbidity, we assessed physical function in mice treated with D+Q or V monthly until death. Despite the longer remaining lifespan in the D+Q-treated mice, physical function in their last 2 months of life was not lower compared to V-treated mice in either males or females (Fig. 6m and Supplementary Fig.14c,d). At autopsy, the prevalence of several age-related diseases, tumor burden, and cause of death, was not statistically different between D+Q- and V-treated mice in either males or females (Fig. 6n and Supplementary Fig.15). Thus, orally-active senolytic drugs, which reduce the burden of senescent and possibly other cells that have exaggerated inflammatory cytokine production coupled with dependence on pro-survival SCAP pathways, can increase post-treatment lifespan without causing prolonged morbidity in mice, even when administered late in life.

Discussion

Our study shows that healthspan and lifespan are curtailed by increased senescent cell abundance and, conversely, are enhanced by reducing pro-inflammatory, SCAP-dependent senescent cell burden in mice, even late in life. Collectively, evidence for a causal role of such senescent cells in physical dysfunction satisfies a modified set of Koch's postulates[34]: 1) senescent cell burden[14] and physical dysfunction[5] are associated with each other and aging; 2) transplanting small numbers of senescent cells into young mice that have few endogenous senescent cells is sufficient to cause physical dysfunction that lasts for months; 3) senolytics prevent and alleviate this senescent cell transplantation-induced physical dysfunction in young mice; 4) clearing senescent cells alleviates physical dysfunction and increases remaining lifespan in old mice; and 5) inducing senescence locally in the lung impaired physical function, while clearing senescent cells improved physical function in a bleomycin-induced pulmonary fibrosis mouse model[25]. Notably, we determined that the total cell number in recipient adipose tissue is approximately 350 million. Several studies have shown that the percentage of senescent cells in adipose tissue from aged animals can be up to 2-10%[14,15,20], indicating there might be at least 7 million endogenous senescent cells in adipose tissue of aged mice. While other mechanisms might contribute, one reason why such a small number (0.5-1 million) of transplanted senescent cells could cause systemic dysfunction is spread of senescence and inflammation locally and to distant tissues.

We used preadipocytes for transplantation since these cells appear to be less susceptible to immune rejection than other cell types[26], a reason for their increasing clinical use in cell transplantation studies. To test further if there is a role of immune rejection in the physical dysfunction caused by SEN cell transplantation, we performed autologous transplantation and also transplanted human SEN cells into immuno-deficient (SCID-beige) mice. SEN cells induced essentially identical physical dysfunction in both of these settings in which immune rejection is greatly reduced. These points, together with our finding that transplanted SEN and CON cells disappear at the same rate following transplantation, plus the long-lasting phenotypes caused by transplanting SEN cells, indicate that immune-rejection or transient

"sickness" caused by transplantation might not be a primary cause for the physical dysfunction we found. The SCID-beige mouse senescent cell transplantation model could pave the way for testing the effects of other SEN cell types that are more immunogenic than preadipocytes or autologous cells in future studies.

We originally discovered that D and Q are senolytic agents by using a hypothesis-driven bioinformatics approach. This approach was based on the hypotheses that senescent cells depend on pro-survival pathways to defend themselves against their pro-apoptotic microenvironment and that disabling these pathways would therefore selectively kill senescent cells[35]. That D+Q can specifically kill senescent cells in human adipose tissue is supported by the following evidence: 1) We previously showed that D+Q induce apoptosis only in senescent human cells, rather than non-senescent control cells *in vitro*[35]; 2) D+Q significantly decreased senescent cells by three different assessments, while D+Q did not reduce the overall number of cells in adipose tissue; and 3) Secretion of two major adipokines was not reduced by D+Q, effectively ruling out non-specific effects on secretion or cell viability. We believe these data indicate it is unlikely that non-specific cellular toxicity occurs as a result of D+Q. Of note, we showed the effectiveness of senolytics in targeting naturally-occurring senescent cells in human adipose tissue explants collected from obese subjects. Although similar to aging, obesity is highly associated with increased senescent cell burden[27,32]. In future studies the efficacy of senolytics in tissues from older humans needs to be compared to that in explants from obese subjects.

We found that D+Q has little direct effect on macrophages. However, it is unlikely that the substantial reduction of pro-inflammatory cytokine secretion following D+Q was due to elimination of senescent cells alone. Interestingly, we found that senescent cells can induce adipose tissue cytokine production, potentially amplifying inflammation. By clearing senescent cells, this possible amplification of inflammation could be attenuated in adipose tissue, which includes macrophages. Based on these findings, we speculate that by decreasing senescent cell abundance, reduced inflammatory activity in adipose tissue could ensue and contribute to the reduction of inflammation after D+Q exposure, as well as to decreased spread of senescence.

Reducing highly $p16^{Ink4a+}$-expressing cells, some of which are senescent, in *INK-ATTAC* transgenic mice starting from mid-adulthood (age 12 months) reportedly extends median lifespan[49]. In our study, administration of D+Q or AP20187 under the same conditions to wild-type or *INK-ATTAC* mice was started at age 24-27 months. Unlike D+Q, AP20187 did not enhance late life survival. One reason could be that senolytics act by disabling SCAPs, a mechanism of action that is distinct from that in *INK-ATTAC* mice, in which highly $p16^{Ink4a}$-expressing cells are targeted. We chose old age (24-27 months) rather than middle age (12 months) to start treatment for several reasons. Firstly, twelve month old mice are roughly equivalent to 40 year old humans, while 24 month old mice are equivalent to 75 year olds. We felt that beginning at 24 months of age is potentially a more translatable scenario. Secondly, AP20187 targets $p16^{Ink4a+}$ cells, some of which are senescent, but others of which are not[52,53] (*e.g.*, pancreatic β-cells, macrophages, *etc.*). As 12 month old mice have very few detectible senescent cells in adipose tissue while 24 month old animals do[20], beginning AP20187 administration at 12 months of age could have targeted a higher

proportion of $p16^{Ink4a+}$ cells that are not senescent compared to initiating treatment at 24 months of age, when senescent cells are readily detectible in multiple tissues. Thirdly, treating *INK-ATTAC* mice from 12-month-old mice led to an increase in median rather than maximum survival. This is consistent with our finding here that AP20187 did not detectibly increase late life survival. On the other hand, we show here that by initiating senolytics in later life, late life survival is actually increased.

Age-related diseases were delayed as a group in old male and female mice treated with D+Q compared to vehicle-treated controls. There was no one disease that was delayed or prevented that alone accounted for this increase in survival. In further support of the hypothesis that senescent cells participate in predisposition to age-related dysfunction, we found that the converse is also the case. Age-related diseases occurred earlier as a group in SEN cell-transplanted mice, coupled with shorter survival, than in control non-SEN cell-transplanted mice. No one disease accounted for this decreased survival. These findings are consistent with the geroscience hypothesis: by targeting a fundamental aging process, such as cellular senescence, age-related disorders will be delayed as a group, with no one condition predominating.

Q has been found to alleviate a variety of disorders through diverse mechanisms of action[54], almost all of which have been studied with uninterrupted dosing, resulting in Q being continuously present, consistent with the presumption that Q acts on specific enzymes or pathways to achieve these effects. However, in our study, we administered D+Q intermittently. D and Q both have short elimination half-lives[44,45], supporting the possibility that their beneficial effects on late-life function and survival were at least partially due to a mechanism that persists long after the drugs are no longer present, such as senescent cell elimination. D can have side effects, occasionally including serious ones such as pulmonary edema, which can occur after 8-48 months of daily administration[55]. While recognizing side effects of drugs in mice often differ substantially from humans, in our study mice given D+Q intermittently lived longer and had improved physical function compared to V-treated mice. When they eventually died, the mice did not have pathologies at autopsy and by histological analysis that differed substantially from V-treated mice. Possibly, intermittent treatment with senolytics may serve to reduce potential side effects[56], an important consideration in the frail elderly, a population vulnerable to adverse drug reactions. We emphasize that preclinical studies to search for potential toxicities and optimized regimens are required before contemplating trials in relatively healthy humans. A search for possible side effects of senolytics as a class and of individual senolytics is especially important.

Our study provides proof-of-concept evidence indicating that targeting senescent cells can improve both health- and life-span in mice. Due to the role of senescent cells in inducing physical dysfunction in mice demonstrated here (with some similarity to human frailty[4,31,51]), senolytics might prove to be effective in alleviating physical dysfunction and resulting loss of independence in older human subjects, depending on whether these agents turn out to be safe and effective in clinical trials. Depending on the outcomes of such ongoing (ClinicalTrials.gov identifier: NCT02848131) and future pre-clinical and clinical studies, intermittent administration of senolytics, including newer agents such as optimized derivatives of D+Q, could possibly find use in enhancing healthspan and remaining survival

not only in older subjects, but also in other individuals, such as cancer survivors treated with senescence-inducing radiation or chemotherapy[57].

Online Methods

Mouse Models and Drug Treatments

All animal experiments were performed according to protocols approved by the Institutional Animal Care and Use Committee (IACUC) at Mayo Clinic. Wild-type C57BL/6 mice were obtained from the National Institute on Aging (NIA) and maintained in a pathogen-free facility at 23-24°C under a 12 hour light, 12 hour dark regimen with free access to normal chow diet (standard mouse diet with 20% protein, 5% fat [13.2% fat by calories], and 6% fiber; Lab Diet 5053, St. Louis, MO) and water. Quarterly testing was negative for the following pathogens: *Clostridium piliforme*, *Mycoplasma pulmonis*, cilia-associated respiratory (CAR) bacillus, ectromelia, rotavirus (EDIM), Hantaan, K virus, lymphocytic choriomeningitis virus (LCMV), lactate dehydrogenase elevating virus (LDEV), mouse adenovirus 1 and 2, mouse cytomegalovirus (MCMV), mouse hepatitis virus (MHV), minute virus of mice (MVM), mouse parvovirus (MPV), mouse thymic virus (MTV), Polyoma, pneumonia virus of mice (PVM), REO3, Sendai virus, myocoptes, Theiler's murine encephalomyelitis virus (TMEV), *Encephalitozoon cuniculi*, *Aspiculuris tetraptera*, *Radfordia/Myobia*, and *Syphacia obvelata*. All mice were fed normal chow unless otherwise indicated. For high-fat feeding, a 60% (by calories) fat diet (D12492, irradiated; Research Diets, New Brunswick, NJ) was used. All mice were housed in static autoclaved HEPA-ventilated microisolator cages (27 × 16.5 × 15.5 cm) with autoclaved Enrich-o'Cobs (The Andersons Incorporated) as bedding. Cages and bedding were changed bi-weekly. Cages were opened only in class II biosafety cabinets.

Luciferase transgenic C57BL/6 mice were obtained from the Jackson Laboratory (Bar Harbor, ME; Stock No: 025854) that express firefly luciferase driven by the constitutively-active CAG promoter in most tissues. SCID beige mice (C.B.-17/IcrHsd-*Prkdc*^{scid} *Lyst*$^{bg\text{-}J}$) were purchased from ENVIGO (Huntingdon, Cambridgeshire, United Kingdom). T.T., J.L.K., J. van Deursen (Mayo), and D. Baker (Mayo) devised the strategy for and developed *INK-ATTAC* mice[49]. In *INK-ATTAC* mice, the expression of ATTAC, a construct previously reported[58], is driven by a senescence-activated p16^{Ink4a} promotor sequence. AP20187, a drug that does not appear to affect cells lacking the ATTAC fusion protein, cross-links the mutated FKBP components of ATTAC, allowing the caspase-8 components to be activated through dimerization, leading to apoptosis of cells with high p16^{Ink4a} expression, which includes many senescent cells. These *INK-ATTAC* mice were then bred onto a C57BL/6 background (in the Van Deursen laboratory), genotyped (in the Kirkland laboratory), and aged to 24-27 months (in the Kirkland laboratory). For the lifespan study, AP20187 (B/B homodimerizer, 10mg/kg) was injected intraperitoneally into *INK-ATTAC*$^{+/-}$ or wild-type mice daily for 3 consecutive days during each treatment course. We repeated these 3 day treatment courses every 2 weeks. *INK-ATTAC*$^{+/-}$ and wildtype mice (24-27 months old) were age-matched littermates. AP20187 was purchased from Clontech (Mountain View, CA). For all dasatinib+quercetin (D+Q) treatments, D (5mg/kg, drug/body weight) and Q (50mg/kg) were administrated by oral gavage in 100-150 μL 10% PEG400. For treating 20-

month-old mice, D+Q was delivered either once monthly or every 2 weeks, with essentially identical effects. For the lifespan study, 24-27-month-old mice were treated with D+Q or V for 3 consecutive days every 2 weeks. D was purchased from LC Laboratories (Woburn, MA). Q and doxorubicin were purchased from Sigma-Aldrich (St Louis, MO). All other reagents were purchased from Thermo Fisher Scientific (Waltham, MA) unless indicated otherwise.

Lifespan Studies

For cell transplantation studies, 16-month-old male C57BL/6 mice were obtained from the National Institute on Aging (NIA). Mice were housed 4-5 per cage. Mice were sorted using body weight from low to high. Next, either SEN or CON transplant treatments were assigned to every other mouse using a random number generator, with the intervening mice being assigned to the other treatment, so that pairs of SEN- and CON-transplanted mice were matched by weight. After 1 month of acclimation, cells were transplanted at age 17 months. Physical function tests were performed 1 month after transplantation, at age 18 months. After that, no further tests were performed on these mice except for checking their cages. The earliest death occurred approximately 2 months after the last physical function test. For D+Q studies, 19-21-month-old C57BL/6 mice were obtained from the NIA. Mice were housed 3-5 per cage. As with the transplanted mice, animals were sorted based body weight and randomly assigned to D+Q or V treatment by a person unaware of the study design. Starting at age 24-27 months, mice were treated every 2 weeks with D+Q or V by oral gavage for 3 consecutive days. Some of the mice were moved from their original cages during the course of the study to minimize single cage-housing stress. RotaRod and hanging tests were conducted monthly because these tests are sensitive and non-invasive. We euthanized mice and scored them as having died if they exhibited more than one of the following signs[59]: 1) unable to drink or eat; 2) reluctant to move even with stimulus; 3) rapid weight loss; 4) severe balance disorder; or 5) bleeding or ulcerated tumor. No mouse was lost due to fighting, accidental death, or dermatitis. The Cox proportional hazard model was used for survival analyses.

Postmortem Pathological Examination

Cages were checked every day and dead mice were removed from cages. Within 24 hours, the dead bodies were opened (abdominal cavity, thoracic cavity, and skull) and preserved in 10% formalin individually for at least 7 days. Decomposed or disrupted bodies were excluded. The preserved bodies were shipped to Dr. Yuji Ikeno for pathological examination. The pathological assessment has been described previously [60]. Briefly, tumor burden (the sum of different types of tumors in each mouse), disease burden (the sum of different histopathological changes of major organs in each mouse), severity of each lesion, and inflammation (lymphocytic infiltrate) were assessed.

Cell Culture

Mouse preadipocytes (also termed adipose-derived stem cells or adipocyte progenitors) were isolated as described previously[61]. Briefly, after euthanasia, inguinal fat depots were removed under sterile conditions from mice. Adipose tissue was cut into small pieces, digested in collagenase (1mg/ml) for 60 min at 37°C, and then filtered through a 100 μm

nylon mesh. After centrifugation at 1,000 rpm for 10 min, cell pellets were washed with PBS once and plated in α-MEM containing 10% FBS and antibiotics. After 12 hours, adherent preadipocytes were washed, trypsinized, and replated in order to reduce potential endothelial cell and macrophage contamination. Ear fibroblasts were isolated as described previously[62].

Whole Mouse DNA Determination

All major organs and the whole skeleton from 5-month-old mice, except intestine (to exclude microbiota), were lysed in lysis buffer (100 mM Tris-HCl, pH8.8; 5 mM EDTA, pH8.0; 0.2% SDS; 200 mM NaCl; 100 μg/ml proteinase K) by rotating at 60˚C for 1 week. Most tissues except for some bone were digested. Total DNA per mouse was ~45.5±3.6 mg (mean ± SD; n =3). The molecular weight of whole mouse genome is 1.8×10^{12} Daltons (Da), which is equivalent to $1.8\times10^{12} \times 1.67\times10^{-24}=3\times10^{-12}$g. Therefore, each diploid mouse cell has at least 6×10^{-12}g DNA and a 5-month-old mouse has at least $7\text{-}8\times10^{9}$ diploid cells. Using the same method, we estimate that intraperitoneal adipose tissue from a mouse contains $\sim3.5\text{-}6\times10^{8}$ diploid cells. Based on average body weight, we estimate that there is total of $\sim7.5\text{-}8.7\times10^{9}$ diploid cells throughout the body of a 17-month-old mouse.

Cell Transplantation

To induce senescence in cells to be transplanted, we used radiation or doxorubicin, as opposed to serial passaging because: 1) the radiation and chemotherapy frequently used for treating cancers can be associated with frailty[57]; 2) serially-passaging mouse primary cells can induce spontaneous immortalization of mouse cells, effectively ruling out their use for transplantation[63]; and 3) the SASP of radiation-induced senescent preadipocytes resembles that of serial passaged senescent preadipocytes[14]. Senescence was induced by 10 Gy of cesium radiation or 0.2 mM doxorubicin for 24 hours as described previously[14,15]. We mainly used radiation-induced senescent cells in our studies unless indicated otherwise. We considered these cells to be senescent 20 days after these treatments[14]. More than 85% of cells were senescent based on two assays. Senescent or control cells were collected by trypsinization. Cell pellets were washed with PBS once and re-suspended in PBS for transplantation. Mice were anesthetized using isofluorane and cells were injected intraperitoneally in 150 μl PBS through a 22G needle. We observed that injection using 22G needles did not interfere with the viability of senescent or control cells.

Bioluminescence Imaging

Mice were injected intraperitoneally with 3 mg d-luciferin (Gold Biotechnology, St. Louis, MO) in 200 μl PBS. Mice were anesthetized using isofluorane and bioluminescence images were acquired using a Xenogen Ivis 200 System (Caliper Life Sciences, Hopkinton, MA) according to the manufacturer’s instructions.

Physical Function Measurements

All measurements were performed at least 5 days after the last dose of D+Q treatment. Maximal walking speed was assessed using an accelerating RotaRod system (TSE system, Chesterfield, MO). Mice were trained on the RotaRod for 3 days at speeds of 4, 6, and 8 rpm for 200 seconds on days 1, 2, and 3. On the test day, mice were placed onto the RotaRod and

then started at 4 rpm. The rotating speed was accelerated from 4 to 40 rpm over a 5 min interval. The speed was recorded when the mouse dropped off the RotaRod. Results were averaged from 3-4 trials and normalized to baseline speed. Training was not repeated for mice that had been trained within the preceding 2 months. Forelimb grip strength (N-F/kg) was determined using a Grip Strength Meter (Columbus Instruments, Columbus, OH). Results were averaged over 10 trials. For the hanging test, mice were placed onto a 2 mm thick metal wire, 35 cm above a padded surface. Mice were allowed to grab the wire with their forelimbs only. Hanging time was normalized to body weight as hanging duration (sec) × body weight (g). Results were averaged from 2-3 trials for each mouse. A Comprehensive Laboratory Animal Monitoring System (CLAMS) was used to monitor daily activity and food intake over a 24-hour period (12 hours light and 12 hours dark). The CLAMS system is equipped with an Oxymax Open Circuit Calorimeter System (Columbus Instruments). For treadmill performance, mice were acclimated to a motorized treadmill at an incline of 5° (Columbus Instruments) over 3 days for 5 min each day starting at a speed of 5m/min for 2 min, 7 m/min for 2 min, and then 9 m/min for 1 min. On the test day, mice ran on the treadmill at an initial speed of 5 m/min for 2 min and then the speed was increased by 2 m/min every 2 min until the mice were exhausted. Exhaustion was defined as the inability to return onto the treadmill despite a mild electrical shock stimulus and mechanical prodding. Distance was recorded and total work (kJ) was calculated using the following formula: mass (kg) × g (9.8 m/s^2) × distance (m) × sin(5°).

Real-Time PCR

Trizol was used to extract RNA from tissues. RNA was reverse-transcribed to cDNA using a M-MLV Reverse Transcriptase kit (Thermo Fisher Scientific) following the manufacturer's instructions. TaqMan fast advanced master mix (Thermo Fisher Scientific) was used for real-time PCR. TATA-binding protein (TBP) was used as an internal control. Probes and primers (TBP, Mm01277042_m1; IL-6, Mm00446191_m1; TNF-α, Mm00443260_g1; $p16^{INK4a}$, Mm00494449_m1; $p21^{Cip1}$, Mm04205640_g1) were purchased from Thermo Fisher Scientific.

Testosterone Assay

Circulating testosterone was assayed by liquid chromatography-tandem mass spectrometry (LC-MS/MS) (Agilent Technologies, Santa Clara, CA 95051). Intra-assay coefficients of variation (C.V.) are 7.4%, 6.1%, 9.0%, 2.3%, and 0.9% at 0.65, 4.3, 48, 118, and 832 ng/dL, respectively. Inter-assay C.V.'s are 8.9%, 6.9%, 4.0%, 3.6%, and 3.5% at 0.69, 4.3, 45, 117, and 841 ng/dL, respectively.

Human Adipose Tissue Explants

The protocol was approved by the Mayo Clinic Foundation Institutional Review Board for Human Research. Informed consent was obtained from all subjects. Human adipose tissue was resected during gastric bypass surgery from 8 obese subjects. Two of the subjects were male and 6 were female. Ages of subjects were 45.8±8.2 years (means ± SD; range 36–58). Mean body mass index (BMI) was 45.5±9.1 kg/m^2 (means ± SD; range 38–66). No subject was known to have a malignancy. Greater omental adipose tissue was obtained from each subject. Adipose tissue was cut into small pieces and washed with PBS 3 times. Adipose

tissue was then cultured in medium containing 1 mM sodium pyruvate, 2 mM glutamine, MEM vitamins, MEM non-essential amino acids, and antibiotics with 20 μM Q and 1 μM D or DMSO. After 48 hours, the adipose explants were washed 3 times with PBS. Aliquots of adipose tissue were fixed for immunostaining or SA-βgal assay. The rest of the tissue was maintained in the same medium without drugs for 24 hours to collect conditioned medium (CM) for multiplex protein analysis. For Supplementary Figure 10, CM was collected from senescent (SEN) human primary preadipocytes, non-senescent control (CON) preadipocytes, and blank culture flasks containing no cells (Blank CM). Senescent and control preadipocytes were from the same donor. Human subcutaneous adipose tissue explants were obtained from a lean kidney donor (BMI 26.5 kg/m2; age 43 years) and divided into pieces. These explants were incubated with SEN, CON, or Blank CM for 24 hours. Next, these explants were washed with PBS, and then incubated with fresh medium for conditioning for another 24 hours.

Multiplex Protein Analyses

Pro-inflammatory cytokine and chemokine protein levels in CM were measured using Luminex xMAP technology. The multiplexing analysis was performed using the Luminex™ 100 system (Luminex, Austin, TX) by Eve Technologies Corp. (Calgary, Alberta, Canada). Human multiplex kits were from Millipore (Billerica, MA).

SA-βgal Assay and Immunostaining

Adipose tissue cellular SA-βgal activity was assayed as previously described [14]. TAF immuno-fluorescence *in situ* hybridization was performed as described previously[30]. Briefly, formalin-fixed, paraffin-embedded (FFPE) adipose tissue blocks were cut into 5 μm sections. Sections were de-paraffinized with Histoclear (National Diagnostics, Charlotte, NC) and hydrated using an ethanol gradient. Antigen was retrieved by incubation in 0.01 M, pH 6.0 citrate buffer at 95°C for 10 min. Slides were placed into blocking buffer (goat serum or horse serum 1:60 in 0.1% BSA in PBS) for 60 min at room temperature. Samples were further blocked with Avidin/Biotin (Vector Lab, Burlingame, CA) for 15 min at room temperature. Primary antibody (anti-γH2AX 1:200, Cell Signaling, Danvers, MA, #9718) was applied overnight at 4°C in the blocking buffer. Washed slides were then incubated for 30 min with biotinylated, anti-rabbit secondary antibody (Vector Lab). Finally, Fluorescein Avidin DCS (Vector Lab) was applied for 20 min. For luciferase co-staining, a 2nd primary antibody (anti-luciferase 1:500, Novusbio, Littleton, CO, #NB100-1677SS) was applied overnight at 4°C in blocking buffer. Next, washed slides were incubated with secondary antibody (Alexa Fluor 647 1:500, Thermo Fisher Scientific, # A-21447). Telomeres were then stained by fluorescent *in situ* hybridization (FISH). Slides were fixed with 4% paraformaldehyde for 20 min, dehydrated in an alcohol gradient cascade, and denatured for 10 min at 80°C in hybridization buffer (70% formamide [Sigma-Aldrich], 25 mM $MgCl_2$, 1 M Tris pH 7.2, 5% blocking reagent [Roche, Basel, Switzerland]) with a 2.5 μg/ml Cy-3-labelled telomere-specific (CCCTAA) peptide nucleic acid probe (Panagene, Daejeon, Korea) for 2 hours at room temperature in the dark. After washing, sections were incubated with 4,6-diamidino-2-henylindole (DAPI), mounted, and imaged. In-depth Z-stacking (a minimum of 20 optical slices with 100 × oil objective) was used for imaging. The images were further processed using Huygens (SVI) deconvolution. Immunohistochemical (IHC)

staining was performed by the Pathology Research Core (Mayo Clinic, Rochester, MN) using a Leica Bond RX stainer (Leica, Buffalo Grove, IL). Slides were retrieved for 20 min using Epitope Retrieval 1 (Citrate; Leica) and incubated in Protein Block (Dako, Agilent, Santa Clara, CA) for 5 min. Primary antibodies were diluted in Background Reducing Diluent (Dako) as follows: $p16^{INK4a}$ (rabbit, monoclonal; Abcam, Cambridge, MA) at 1:600, cleaved-caspase 3 (rabbit, polyclonal; Cell Signaling) at 1:200, and F4/80 (rat, monoclonal; Abcam) at 1:500, except for CD68 antibody (mouse, monoclonal; Dako), which was diluted in Bond Diluent (Leica) at 1:200. All primary antibodies were diluted in Background Reducing Diluent (Dako) and incubated for 15 min. The detection system used was a Polymer Refine Detection System (Leica). This system includes the hydrogen peroxidase block, post primary and polymer reagent, DAB, and hematoxylin. Immunostaining visualization was achieved by incubating slides 10 min in DAB and DAB buffer (1:19 mixture) from the Bond Polymer Refine Detection System. Slides were counterstained for 5 min using Schmidt hematoxylin, followed by several rinses in 1x Bond wash buffer and distilled water. Slides were dehydrated using increasing concentrations of ethyl alcohol and cleared by 3 changes of xylene prior to permanent cover-slipping in xylene-based medium.

Statistical Analysis

GraphPad Prism 7.0 was used for most statistical analyses. Two-tailed Student's *t*-tests were used to estimate statistically significant differences between two groups. One-way analysis of variance (ANOVA) with Tukey's *post-hoc* comparison was used for multiple comparisons. Pearson's correlation coefficients were used to test correlations. As mice were obtained in several cohorts and grouped in cages, the Cox proportional hazard model was used for survival analyses. The model incorporated sex and age of treatment as fixed effects, and cohorts and initial cage assignment as random effects. Due to the fact that some of mice were moved from their initial cages during the study to minimize single cage housing stress, we also conducted analyses without cage effect. Results between these two analyses did not differ substantially in directionality or statistical significance, strengthening confidence in our results. Survival analysis was performed using statistical software R (version 3.4.1; library "coxme"). Investigators were blinded to allocation during most of experiments and outcome assessments. We used baseline body weight to assign animals to experimental groups (to achieve similar body weight between groups), so only randomization within groups matched by body weight was conducted. We determined the sample size based on our previous experiments, so no statistical power analysis was used. Values are presented as mean ± SEM unless otherwise indicated, with $P < 0.05$ considered to be significant. All replicates in this study were independent biological replicates, which came from different biological samples.

Data Availability

Detailed information on experimental design and reagents is available in the accompanying **Life Sciences Reporting Summary**. Source data are available for Figures 1–6. Reasonable requests for other data presented in this manuscript will be honored by the corresponding authors.

Supplementary Material

Refer to Web version on PubMed Central for supplementary material.

Acknowledgments

The authors are grateful to J. L. Armstrong and L. Thesing for administrative assistance, M. Mahlman for obtaining human adipose tissue samples, Z. Aversa for help with muscle analysis, the Pathology Research Core Lab at Mayo Clinic-Rochester for histology studies, and C. Guo for overall support. This work was supported by the Connor Group (JLK) and Robert J. and Theresa W. Ryan (JLK), NIH grants AG13925 (JLK), AG49182 (JLK), DK50456 (Adipocyte Subcore, JLK), AG46061 (AKP), AG004875 (SK), AG048792 (SK), AR070241 (JNF), AR070281 (MMW), AG13319 (YI, GBH), AG050886 (DBA), AG043376 (PDR, LJN), AG056278 (PDR, LJN), and AG044376 (LJN), a Glenn/American Federation for Aging Research (AFAR) BIG Award (JLK), the Glenn Foundation (LJN), and the Ted Nash Long Life and Noaber Foundations (JLK). MX received the Glenn/AFAR Postdoctoral Fellowship for Translational Research on Aging and a Irene Diamond Fund/AFAR Postdoctoral Transition Award in Aging.

References

1. Crimmins EM. Lifespan and Healthspan: Past, Present, and Promise. Gerontologist. 2015; 55:901–911. [PubMed: 26561272]
2. Fries JF. Aging, natural death, and the compression of morbidity. N Engl J Med. 1980; 303:130–135. [PubMed: 7383070]
3. Michaud M, et al. Proinflammatory cytokines, aging, and age-related diseases. J Am Med Dir Assoc. 2013; 14:877–882. [PubMed: 23792036]
4. Fried LP, et al. Frailty in older adults: evidence for a phenotype. J Gerontol A Biol Sci Med Sci. 2001; 56:M146–156. [PubMed: 11253156]
5. Collard RM, Boter H, Schoevers RA, Oude Voshaar RC. Prevalence of frailty in community-dwelling older persons: a systematic review. Journal of the American Geriatrics Society. 2012; 60:1487–1492. [PubMed: 22881367]
6. Song X, Mitnitski A, Rockwood K. Prevalence and 10-year outcomes of frailty in older adults in relation to deficit accumulation. Journal of the American Geriatrics Society. 2010; 58:681–687. [PubMed: 20345864]
7. Xue QL. The frailty syndrome: definition and natural history. Clinics in geriatric medicine. 2011; 27:1–15. [PubMed: 21093718]
8. Tchkonia T, Zhu Y, van Deursen J, Campisi J, Kirkland JL. Cellular senescence and the senescent secretory phenotype: therapeutic opportunities. The Journal of clinical investigation. 2013; 123:966–972. [PubMed: 23454759]
9. Campisi J, d'Adda di Fagagna F. Cellular senescence: when bad things happen to good cells. Nat Rev Mol Cell Biol. 2007; 8:729–740. [PubMed: 17667954]
10. Wiley CD, et al. Mitochondrial Dysfunction Induces Senescence with a Distinct Secretory Phenotype. Cell Metab. 2016; 23:303–314. [PubMed: 26686024]
11. Wang C, et al. DNA damage response and cellular senescence in tissues of aging mice. Aging Cell. 2009; 8:311–323. [PubMed: 19627270]
12. Zhu Y, Armstrong JL, Tchkonia T, Kirkland JL. Cellular senescence and the senescent secretory phenotype in age-related chronic diseases. Current opinion in clinical nutrition and metabolic care. 2014; 17:324–328. [PubMed: 24848532]
13. Coppe JP, et al. Senescence-associated secretory phenotypes reveal cell-nonautonomous functions of oncogenic RAS and the p53 tumor suppressor. PLoS Biol. 2008; 6:2853–2868. [PubMed: 19053174]
14. Xu M, et al. JAK inhibition alleviates the cellular senescence-associated secretory phenotype and frailty in old age. Proc Natl Acad Sci U S A. 2015; 112:E6301–6310. [PubMed: 26578790]
15. Xu M, et al. Targeting senescent cells enhances adipogenesis and metabolic function in old age. Elife. 2015; 4:e12997. [PubMed: 26687007]

16. Xu M, et al. Transplanted Senescent Cells Induce an Osteoarthritis-Like Condition in Mice. J Gerontol A Biol Sci Med Sci. 2017; 72:780–785. [PubMed: 27516624]
17. Palmer AK, et al. Cellular Senescence in Type 2 Diabetes: A Therapeutic Opportunity. Diabetes. 2015; 64:2289–2298. [PubMed: 26106186]
18. Chang J, et al. Clearance of senescent cells by ABT263 rejuvenates aged hematopoietic stem cells in mice. Nature medicine. 2016; 22:78–83.
19. Childs BG, et al. Senescent intimal foam cells are deleterious at all stages of atherosclerosis. Science. 2016; 354:472–477. [PubMed: 27789842]
20. Baker DJ, et al. Naturally occurring p16(Ink4a)-positive cells shorten healthy lifespan. Nature. 2016; 530:184–189. [PubMed: 26840489]
21. Xu M, Tchkonia T, Kirkland JL. Perspective: Targeting the JAK/STAT pathway to fight age-related dysfunction. Pharmacol Res. 2016; 111:152–154. [PubMed: 27241018]
22. Bitto A, et al. Transient rapamycin treatment can increase lifespan and healthspan in middle-aged mice. Elife. 2016; 5
23. Tchkonia T, et al. Mechanisms and metabolic implications of regional differences among fat depots. Cell Metab. 2013; 17:644–656. [PubMed: 23583168]
24. Farr JN, et al. Identification of Senescent Cells in the Bone Microenvironment. J Bone Miner Res. 2016; 31:1920–1929. [PubMed: 27341653]
25. Schafer MJ, et al. Cellular senescence mediates fibrotic pulmonary disease. Nature communications. 2017; 8:14532.
26. Ryan JM, Barry FP, Murphy JM, Mahon BP. Mesenchymal stem cells avoid allogeneic rejection. J Inflamm (Lond). 2005; 2:8. [PubMed: 16045800]
27. Tchkonia T, et al. Fat tissue, aging, and cellular senescence. Aging Cell. 2010; 9:667–684. [PubMed: 20701600]
28. Acosta JC, et al. A complex secretory program orchestrated by the inflammasome controls paracrine senescence. Nature cell biology. 2013; 15:978–990. [PubMed: 23770676]
29. Nelson G, et al. A senescent cell bystander effect: senescence-induced senescence. Aging Cell. 2012; 11:345–349. [PubMed: 22321662]
30. Hewitt G, et al. Telomeres are favoured targets of a persistent DNA damage response in ageing and stress-induced senescence. Nature communications. 2012; 3:708.
31. Walston J, et al. The physical and biological characterization of a frail mouse model. J Gerontol A Biol Sci Med Sci. 2008; 63:391–398. [PubMed: 18426963]
32. Schafer MJ, et al. Exercise Prevents Diet-Induced Cellular Senescence in Adipose Tissue. Diabetes. 2016; 65:1606–1615. [PubMed: 26983960]
33. Mosier DE, Stell KL, Gulizia RJ, Torbett BE, Gilmore GL. Homozygous scid/scid;beige/beige mice have low levels of spontaneous or neonatal T cell-induced B cell generation. J Exp Med. 1993; 177:191–194. [PubMed: 8418200]
34. Kirkland JL, Tchkonia T. Cellular Senescence: A Translational Perspective. EBioMedicine. 2017
35. Zhu Y, et al. The Achilles' heel of senescent cells: from transcriptome to senolytic drugs. Aging Cell. 2015; 14:644–658. [PubMed: 25754370]
36. Stern JH, Rutkowski JM, Scherer PE. Adiponectin, Leptin, and Fatty Acids in the Maintenance of Metabolic Homeostasis through Adipose Tissue Crosstalk. Cell Metab. 2016; 23:770–784. [PubMed: 27166942]
37. Farmer SR. Transcriptional control of adipocyte formation. Cell Metab. 2006; 4:263–273. [PubMed: 17011499]
38. Reuben DB, Judd-Hamilton L, Harris TB, Seeman TE. The associations between physical activity and inflammatory markers in high-functioning older persons: MacArthur Studies of Successful Aging. Journal of the American Geriatrics Society. 2003; 51:1125–1130. [PubMed: 12890077]
39. Cohen HJ, Pieper CF, Harris T, Rao KM, Currie MS. The association of plasma IL-6 levels with functional disability in community-dwelling elderly. J Gerontol A Biol Sci Med Sci. 1997; 52:M201–208. [PubMed: 9224431]
40. Beyer I, et al. Inflammation-related muscle weakness and fatigue in geriatric patients. Exp Gerontol. 2012; 47:52–59. [PubMed: 22032874]

41. Lu Y, et al. Inflammatory and immune markers associated with physical frailty syndrome: findings from Singapore longitudinal aging studies. Oncotarget. 2016; 7:28783–28795. [PubMed: 27119508]
42. Kao TW, et al. Examining how p16(INK4a) expression levels are linked to handgrip strength in the elderly. Sci Rep. 2016; 6:31905. [PubMed: 27549351]
43. Justice JN, et al. Cellular senescence biomarker p16INK4a+ cell burden in thigh adipose is associated with poor physical function in older women. J Gerontol A Biol Sci Med Sci. 2017
44. Christopher LJ, et al. Metabolism and disposition of dasatinib after oral administration to humans. Drug metabolism and disposition: the biological fate of chemicals. 2008; 36:1357–1364. [PubMed: 18420784]
45. Graefe EU, et al. Pharmacokinetics and bioavailability of quercetin glycosides in humans. Journal of clinical pharmacology. 2001; 41:492–499. [PubMed: 11361045]
46. Roos CM, et al. Chronic senolytic treatment alleviates established vasomotor dysfunction in aged or atherosclerotic mice. Aging Cell. 2016
47. Farr JN, et al. Targeting cellular senescence prevents age-related bone loss in mice. Nature medicine. 2017; 23:1072–1079.
48. Ogrodnik M, et al. Cellular senescence drives age-dependent hepatic steatosis. Nature communications. 2017; 8:15691.
49. Baker DJ, et al. Clearance of p16Ink4a-positive senescent cells delays ageing-associated disorders. Nature. 2011; 479:232–236. [PubMed: 22048312]
50. Srinivas-Shankar U, Wu FC. Frailty and muscle function: role for testosterone? Front Horm Res. 2009; 37:133–149. [PubMed: 19011294]
51. Kane AE, et al. Animal models of frailty: current applications in clinical research. Clin Interv Aging. 2016; 11:1519–1529. [PubMed: 27822024]
52. Hall BM, et al. p16(Ink4a) and senescence-associated beta-galactosidase can be induced in macrophages as part of a reversible response to physiological stimuli. Aging (Albany NY). 2017
53. Helman A, et al. p16-induced senescence of pancreatic beta cells enhances insulin secretion. Nature medicine. 2016
54. Costa LG, Garrick JM, Roque PJ, Pellacani C. Mechanisms of Neuroprotection by Quercetin: Counteracting Oxidative Stress and More. Oxid Med Cell Longev. 2016; 2016:2986796. [PubMed: 26904161]
55. Montani D, et al. Pulmonary arterial hypertension in patients treated by dasatinib. Circulation. 2012; 125:2128–2137. [PubMed: 22451584]
56. Kirkland JL, Tchkonia T, Zhu Y, Niedernhofer LJ, Robbins PD. The Clinical Potential of Senolytic Drugs. Journal of the American Geriatrics Society. 2017
57. Ness KK, et al. Frailty in childhood cancer survivors. Cancer. 2015; 121:1540–1547. [PubMed: 25529481]

Methods-Only References

58. Pajvani UB, et al. Fat apoptosis through targeted activation of caspase 8: a new mouse model of inducible and reversible lipoatrophy. Nature medicine. 2005; 11:797–803.
59. Miller RA, et al. An Aging Interventions Testing Program: study design and interim report. Aging Cell. 2007; 6:565–575. [PubMed: 17578509]
60. Ikeno Y, et al. Housing density does not influence the longevity effect of calorie restriction. The journals of gerontology. Series A, Biological sciences and medical sciences. 2005; 60:1510–1517.
61. Tchkonia T, et al. Increased TNFalpha and CCAAT/enhancer-binding protein homologous protein with aging predispose preadipocytes to resist adipogenesis. Am J Physiol Endocrinol Metab. 2007; 293:E1810–1819. [PubMed: 17911345]
62. Jurk D, et al. Chronic inflammation induces telomere dysfunction and accelerates ageing in mice. Nature communications. 2014; 2:4172.
63. Xu J. Preparation, culture, and immortalization of mouse embryonic fibroblasts. Curr Protoc Mol Biol. 2005:21. Chapter 28, Unit 28.

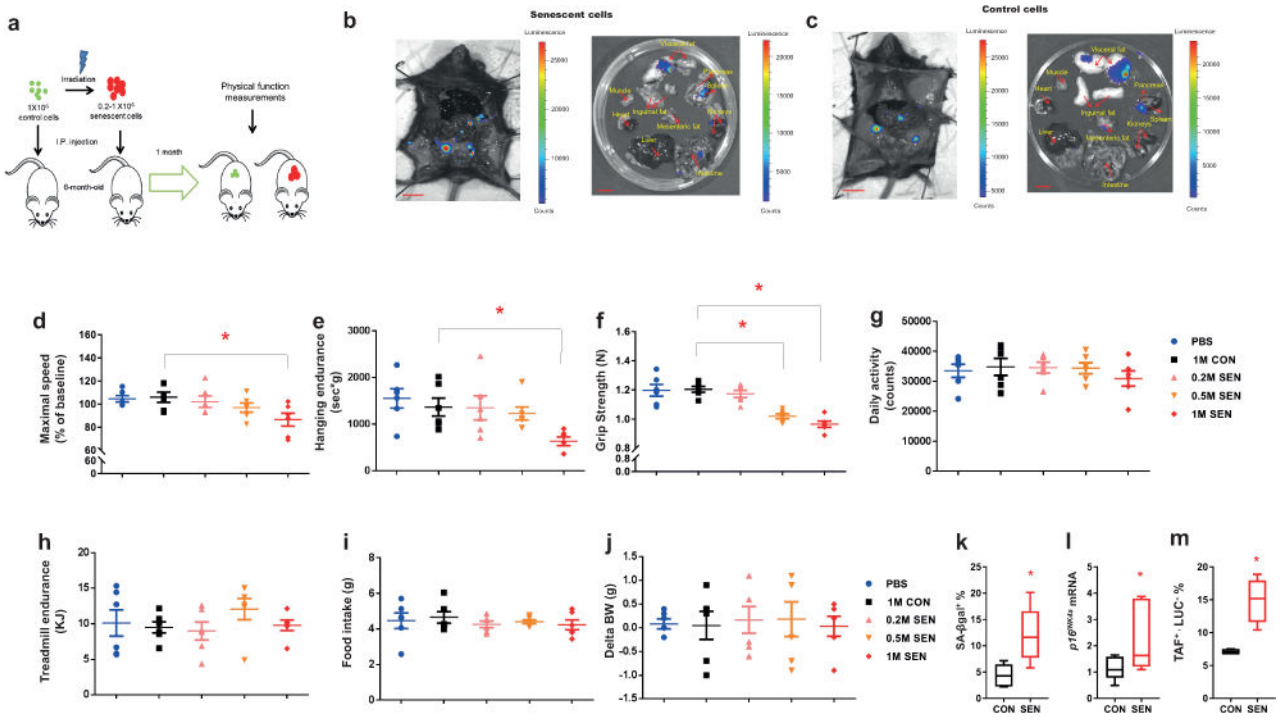

Figure 1.

Transplanting small numbers of senescent cells induces physical dysfunction in younger mice. (**a)** Experimental design for transplantation and physical function measurements. (**b**,**c)** Representative images of LUC activity of various organs from LUC-negative male mice (n = 3) 5 d post-transplantation with SEN (induced by radiation) and CON preadipocytes from LUC-positive transgenic mice. Scale bars, 10 mm. (**d**-**j)** Maximal walking speed (relative to baseline) (**d**), hanging endurance (**e**), grip strength (**f**), daily activity (**g**), treadmill endurance (**h**), food intake (**i**), and change in body weight (BW) (**j**) of 6-month-old male C57BL/6 mice 1 mo after being injected with PBS, 1×10^6 non-senescent control (1M CON), 0.2 x10^6 SEN (0.2M SEN), 0.5×10^6 SEN (0.5M SEN), or 1×10^6 SEN (1M SEN) preadipocytes (n = 6 for all groups). Results are means ± s.e.m. (**k**-**m**). SA-βgal$^+$ cell numbers (n = 6) (**k**), p16^{Ink4a} mRNA levels (n = 7) **(l)**, and cells from recipient mice that were TAF$^+$ (>2 TAFs/nucleus) and LUC$^-$ (n = 4 mice) **(m)** in 6-month-old male wildtype (LUC$^-$) C57BL/6 mice 2 mo after being transplanted with 1×10^6 SEN or CON transgenic constitutively-expressing LUC (LUC$^+$) preadipocytes from transgenic mouse donors. Results are shown as box and whiskers plots, where a box extends from the 25th to 75th percentile with the median shown as a line in the middle, and whiskers indicate smallest and largest values. *P < 0.05; ANOVA with Tukey's *post-hoc* comparison (**d**-**j**) and two-tailed, unpaired Student's t-test (**k**-**m**).

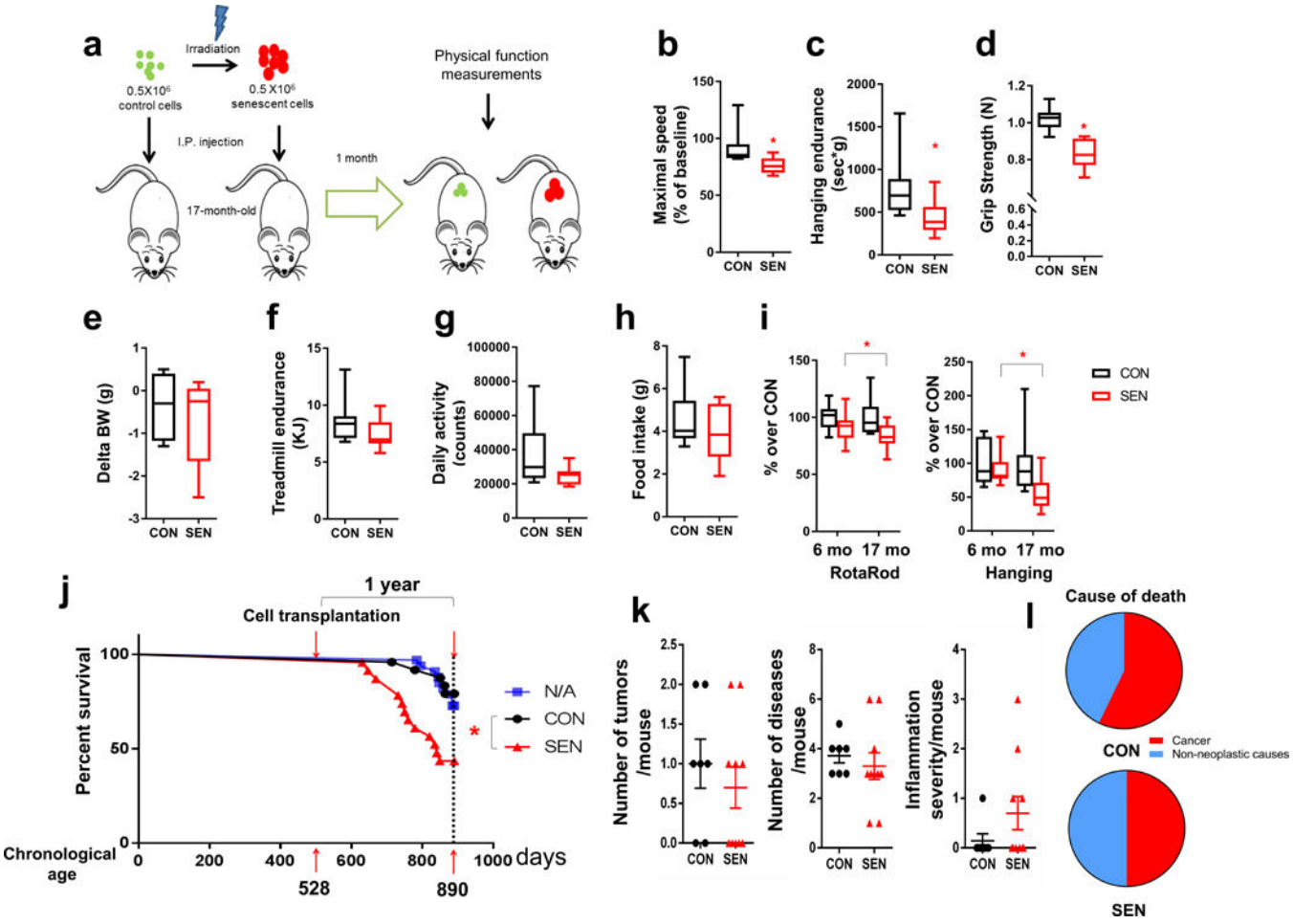

Figure 2.

Aging exacerbates effects of senescent cell transplantation. **(a)** Experimental design for transplantation and physical function measurements. **(b-h)** Maximal walking speed (relative to baseline) (**b**), hanging endurance (**c**), grip strength (**d**), body weight change from baseline (**e**), treadmill endurance (**f**), daily activity (**g**), and food intake (**h**) of 17-month-old male C57BL/6 mice 1 mo after being injected with 0.5×10^6 SEN or CON preadipocytes ($n = 8$ for both groups). **(i)** Percent changes in RotaRod (in 6-month-old mice, $n = 21$ for both SEN and CON; in 17-month-old mice, $n = 22$ for SEN, $n = 20$ for CON) and hanging test (in 6-month-old mice, $n = 6$ for both SEN and CON; in 17-month-old mice, $n = 8$ for both SEN and CON) in mice transplanted with 0.5×10^6 SEN cells relative to the average of mice transplanted with 0.5×10^6 CON cells at both ages. Results are shown as box and whiskers plots, where a box extends from the 25th to 75th percentile with the median shown as a line in the middle, and whiskers indicate smallest and largest values. **(j)** One year survival curves of 17-month-old non-transplanted mice ($n = 33$, N/A) and mice transplanted with 0.5×10^6 SEN ($n = 23$) or CON ($n = 24$) preadipocytes. **(k)** Tumor burden, disease burden, and inflammation at death are shown as means ± s.e.m. after transplanting SEN or CON cells ($n = 10$ for SEN, $n = 7$ for CON). **(l)** Causes of death ($n = 10$ for SEN, $n = 7$ for CON). *$P < 0.05$; Two-tailed unpaired Student's t-test (**b-i**), Cox proportional hazard regression model (**j**) and chi-square and Fisher's exact tests (**l**).

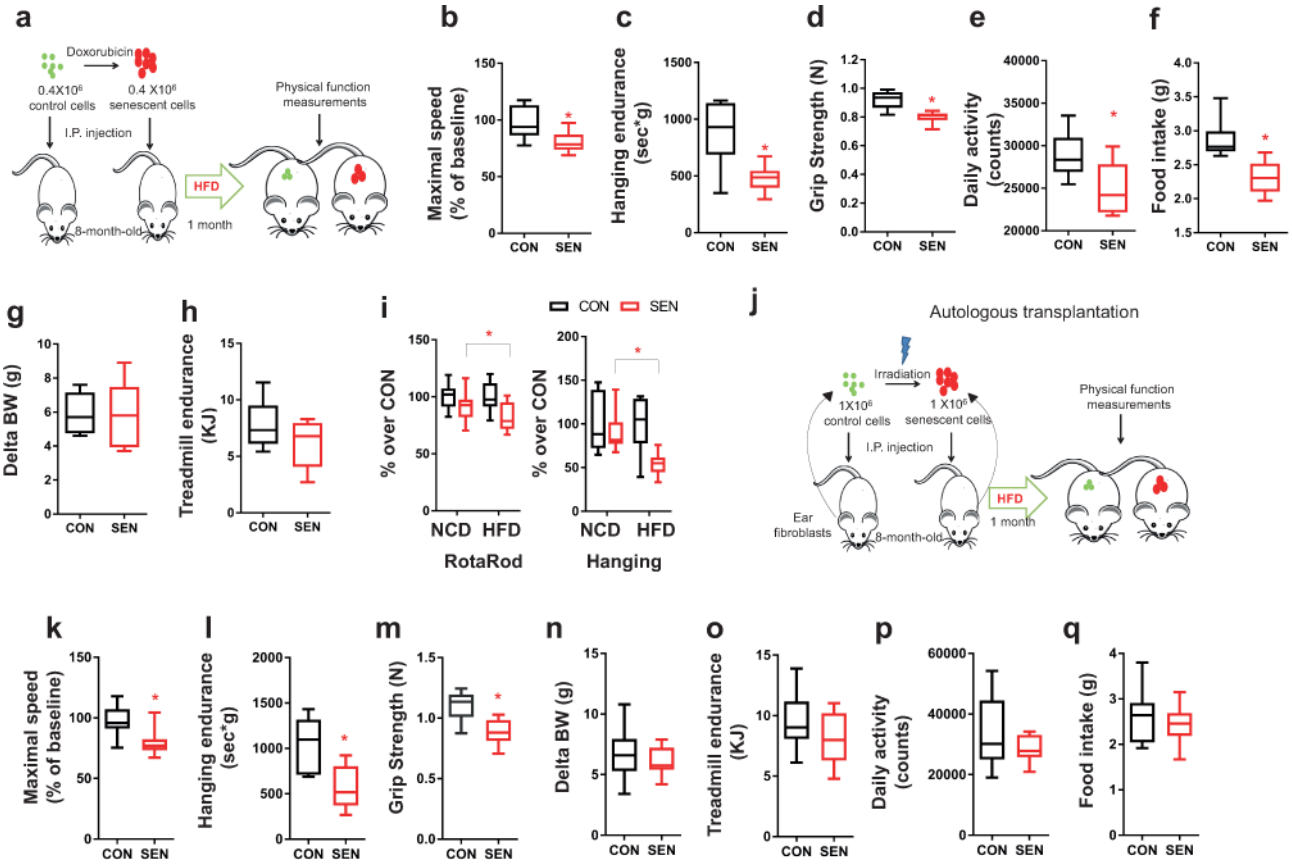

Figure 3.

Senescent cells reduce resilience to metabolic stress in mice. (**a**) Experimental design for transplantation and physical function measurements. (**b**-**h**) Maximal walking speed (relative to baseline) (**b**), hanging endurance (**c**), grip strength (**d**), daily activity (**e**), food intake (**f**), body weight change from baseline (**g**), and treadmill endurance (**h**) of 8-month-old male C57BL/6 mice 1 mo after being on HFD and injected with 0.4 × 10^6 SEN or CON preadipocytes (n = 6 for both groups). **(i)** Percent changes in RotaRod (on NCD, n = 21 for both SEN and CON; on HFD, n = 12 for both SEN and CON) and hanging test (on NCD, n = 6 for both SEN and CON; on HFD, n = 6 for both SEN and CON) in mice transplanted with 0.4-0.5 × 10^6 SEN cells relative to the average of mice transplanted with 0.4-0.5 × 10^6 CON cells. **(j)** Experimental design for transplantation and physical function measurements. **(k-q)** Maximal walking speed (relative to baseline) (**k**), hanging endurance (**l**), grip strength (**m**), body weight change from baseline (**n**), treadmill endurance (**o**), daily activity (**p**), and food intake (**q**) of 8-month-old male C57BL/6 mice 1 mo after being on HFD and injected with 1 × 10^6 SEN or CON autologous ear fibroblasts (n = 10 for both groups). All results are shown as box and whiskers plots, where a box extends from the 25th to 75th percentile with the median shown as a line in the middle, and whiskers indicate smallest and largest values. *P <0.05; Two-tailed unpaired Student's t-tests (**a-q**).

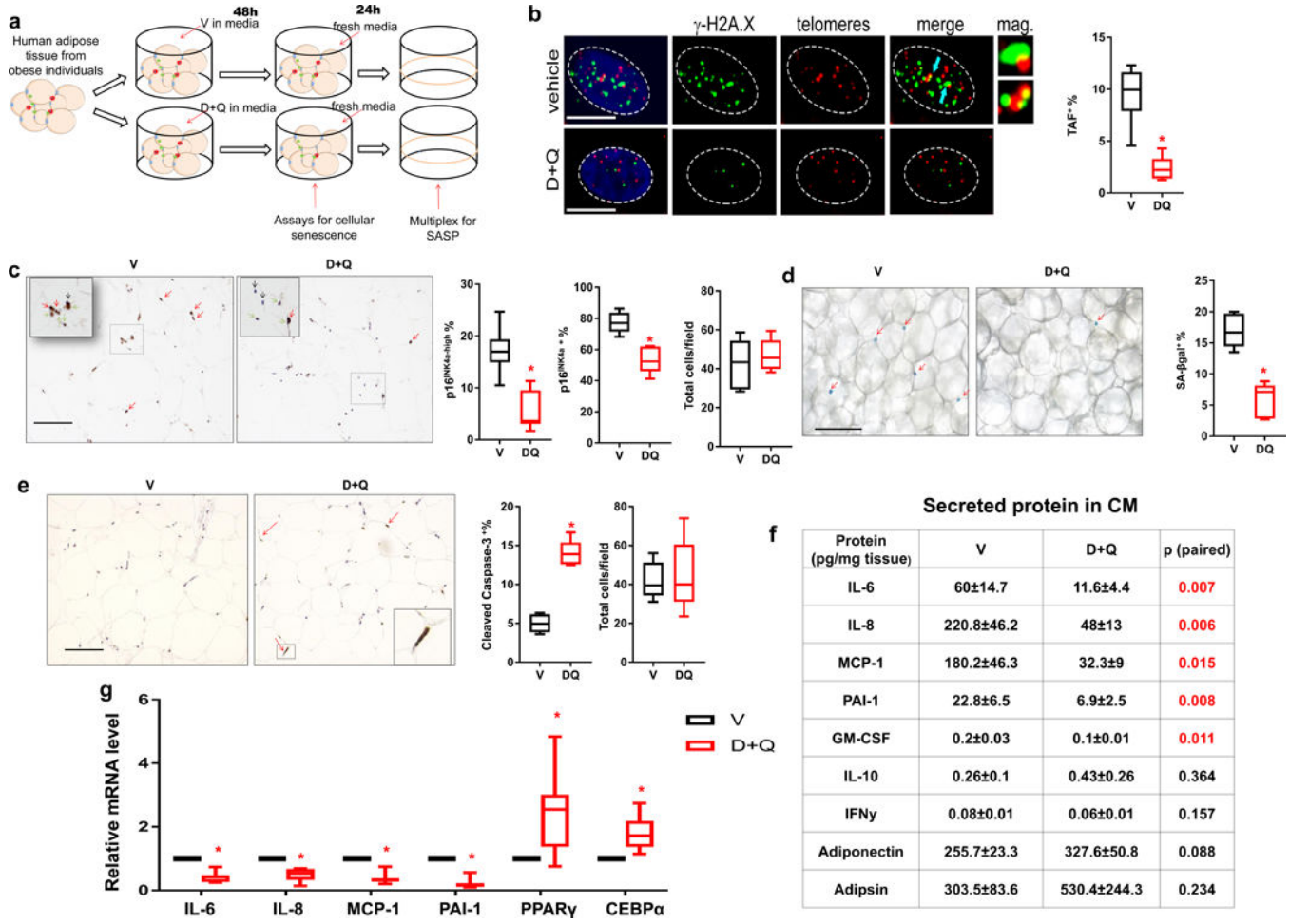

Protein (pg/mg tissue)	V	D+Q	p (paired)
IL-6	60±14.7	11.6±4.4	0.007
IL-8	220.8±46.2	48±13	0.006
MCP-1	180.2±46.3	32.3±9	0.015
PAI-1	22.8±6.5	6.9±2.5	0.008
GM-CSF	0.2±0.03	0.1±0.01	0.011
IL-10	0.26±0.1	0.43±0.26	0.364
IFNy	0.08±0.01	0.06±0.01	0.157
Adiponectin	255.7±23.3	327.6±50.8	0.088
Adipsin	303.5±83.6	530.4±244.3	0.234

Figure 4.

D+Q reduces senescent cell abundance and decreases pro-inflammatory cytokine secretion in human adipose tissue. (**a**) Experimental design. (**b**) Percent TAF^{+} cells (n = 5). Blue arrows indicate TAFs. Scale bars, 5μm. (**c**) Percent p16$^{INK4A\text{-}high}$ cells (red arrows), percent p16^{INK4A+} cells (expressing any detectable level of p16^{INK4A}, green arrows), percent p16^{INK4A-} cells (black arrows), and cell number per field (n = 6). Scale bar, 100μm. (**d**) Percent SA-βgal^{+} cells (red arrows) (n = 6). Scale bar, 100μm. (**e**) Percent cleaved caspase-3^{+} cells (red arrows) (n = 5). Scale bar, 100μm. (**f**) Secreted cytokine and adipokine levels in conditioned media (CM) (n = 8). Results are means ± s.e.m. (**g**) The relative mRNA abundance of key SASP components and markers for adipose tissue function (n = 7). All results are shown as box and whiskers plots, where a box extends from the 25th to 75th percentile with the median shown as a line in the middle, and whiskers indicate smallest and largest values. *P<0.05; Two-tailed Student's t-tests (**a-g**).

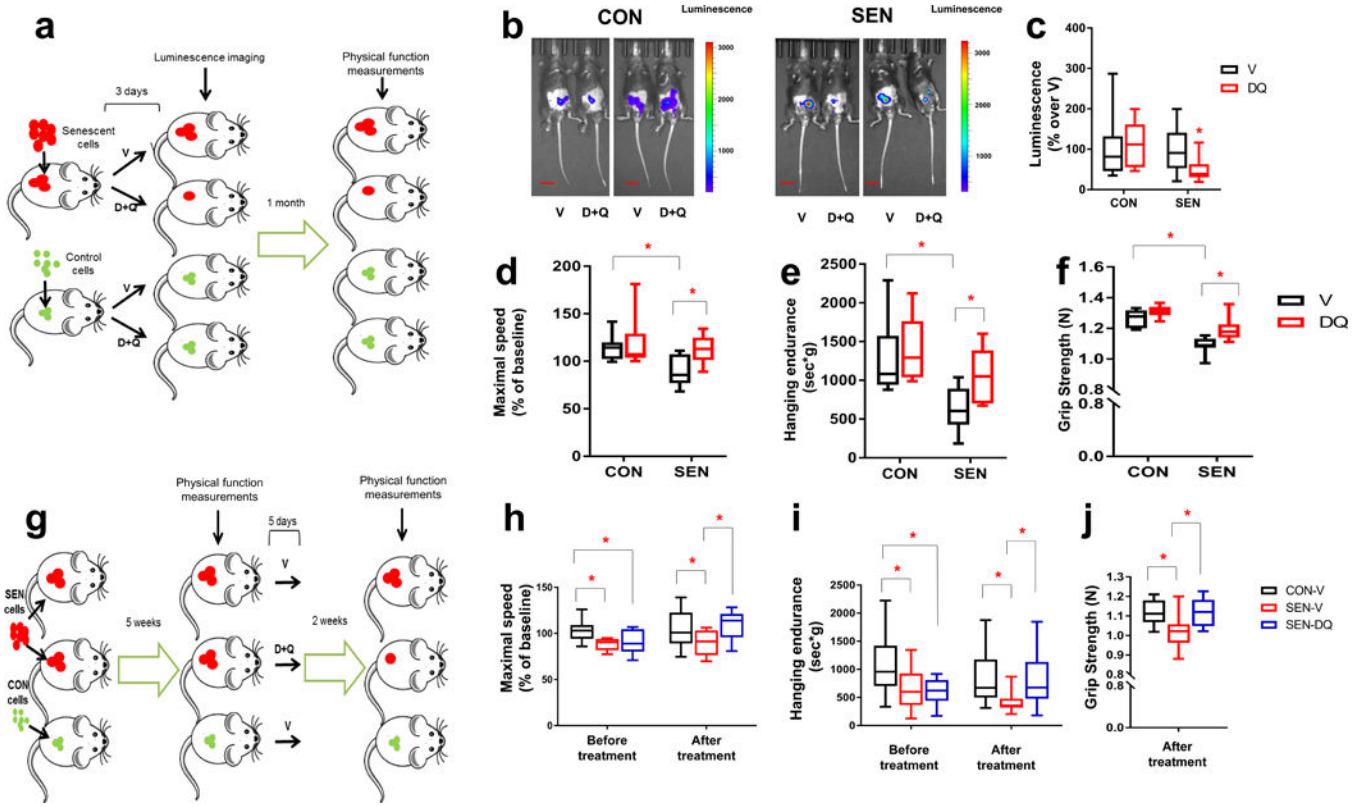

Figure 5.

Eliminating senescent cells both prevents and alleviates physical dysfunction. (**a**) Experimental design for transplantation and physical function measurements. (**b**) Representative images of LUC activity in mice 2 days after the last treatment. Scale bars, 15mm. (**c**) Luminescence of transplanted cells as percent relative to the average of mice treated with V (n =16 for SEN-DQ *vs.* SEN-V; n =13 for CON-DQ *vs.* CON-V). (**d-f**) Maximal walking speed (relative to baseline) (**d**), hanging endurance (**e**), and grip strength (**f**) of 5-month-old male C57BL/6 mice 1 mo after the last drug treatment (n = 7 for SEN-V, CON-V, and SEN-DQ; n = 6 for CON-DQ). (**g**) Experimental design for transplantation and physical function measurements. (**h-j**) Maximal walking speed (relative to baseline) (**h**), hanging endurance (**i**), and grip strength (**j**) of 5-month-old male C57BL/6 mice 2 weeks after the last drug treatment (n = 10 for SEN-DQ and SEN-V; n = 14 for CON-V). All results are shown as box and whiskers plots, where a box extends from the 25th to 75th percentile with the median shown as a line in the middle, and whiskers indicate smallest and largest values. *P <0.05; Two-tailed Student's t-tests (**a-j**).

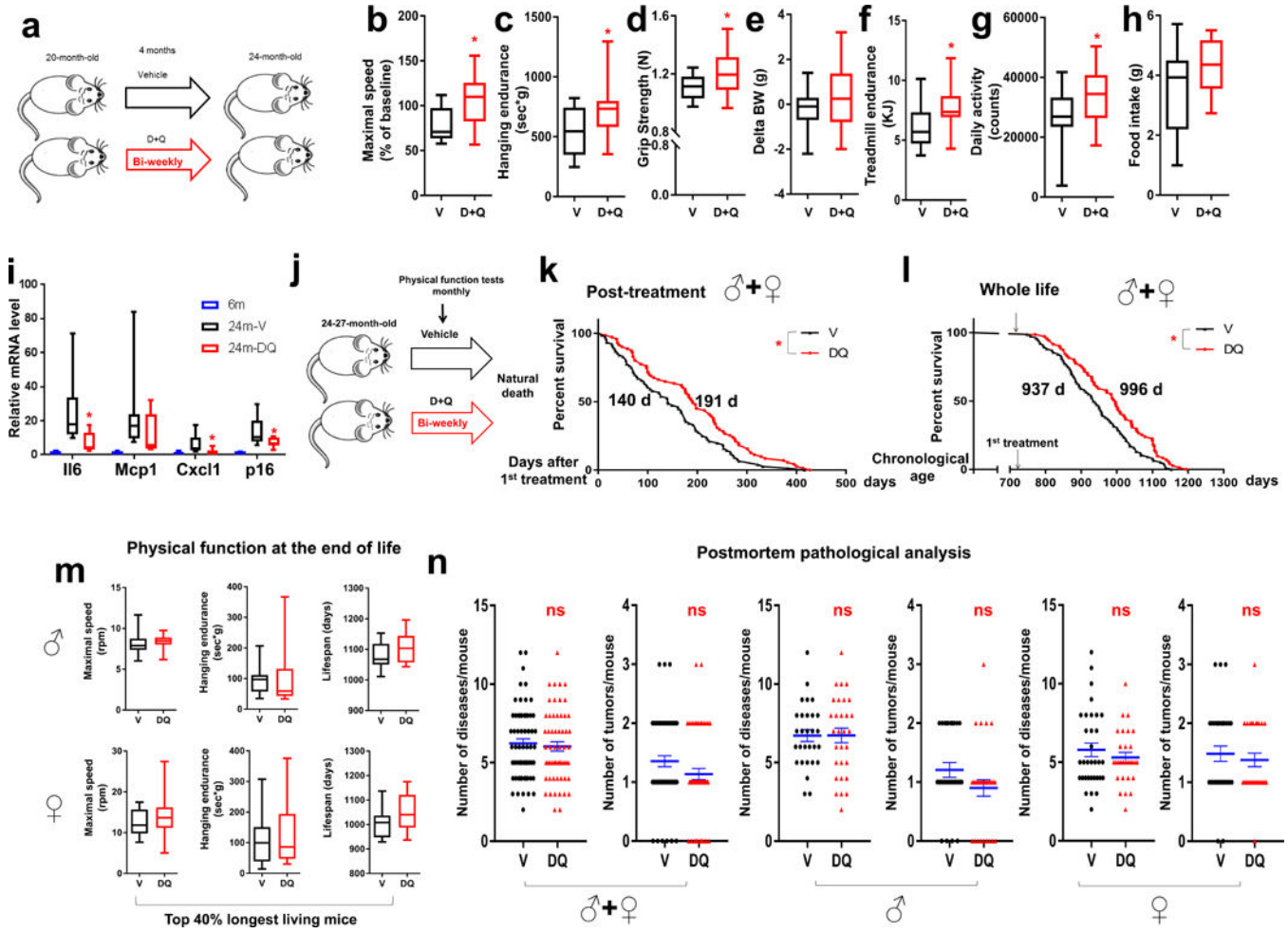

Figure 6.

Senolytics extend both health- and life-span in aged mice. (**a**) Experimental design for physical function measurements in 20-month-old male mice treated with D+Q once every 2 weeks (bi-weekly) for 4 months. (**b**-**h**) Maximal walking speed (relative to baseline) (b), hanging endurance (**c**), grip strength (**d**), body weight change from baseline (**e**), treadmill endurance (**f**), daily activity (**g**), and food intake (**h**) of 20-month-old male C57BL/6 mice 4 mo after drug initiation ($n = 20$ for D+Q; $n = 13$ for V). (**i**) The relative mRNA abundance for target genes of visceral adipose tissue from 6-month-old non-treated (6m, $n = 7$), 24-month-old V-treated (24m-V, $n = 8$), and 24-month-old D+Q-treated (24m-DQ, $n = 8$) mice. (**j**) Experimental design for lifespan analyses. (**k**,**l**) Post-treatment survival curves (**k**) and whole-life survival curves (**l**) of C57BL/6 mice treated bi-weekly with D+Q ($n = 71$; 40 males, 31 females) or V ($n = 76$; 41 males, 35 females) starting at 24-27 months of age. Median survival is indicated for all curves. (**m**) Maximal walking speed and hanging endurance averaged over the last 2 months of life and lifespan for the longest living mice (top 40%) in both groups for both sexes. For male mice, $n = 12$ for D+Q and $n = 12$ for V. For female mice, $n = 13$ for D+Q and $n = 13$ for V. (**n**) Disease burden and tumor burden at death. For both sexes, $n = 59$ for D+Q, $n = 62$ for V. For males, $n = 30$ for D+Q, $n = 29$ for V. For females, $n = 29$ for D+Q, $n = 33$ for V. (**b-i, m**) Results are shown as box and

whiskers plots, where a box extends from the 25th to 75th percentile with the median shown as a line in the middle, and whiskers indicate smallest and largest values. (**n**) Results are shown as mean ± s.e.m. *P <0.05; n.s., not significant; Two-tailed Student's t-tests (**b-i, m-n**) and Cox proportional hazard regression model (**k-l**).